Effects of ion-assisted growth on the layer definition in Cr/Sc multilayers

N. Ghafoor, F. Eriksson, P.O.Å. Persson, L. Hultman and J. Birch

Original publication:

N. Ghafoor, F. Eriksson, P.O.Å. Persson, L. Hultman and J. Birch, Effects of ion-assisted growth on the layer definition in Cr/Sc multilayers, 2008, Thin Solid Films, (516), 6, 982-990.
http://dx.doi.org/10.1016/j.tsf.2007.06.108.

Effects of ion-assisted growth on the layer definition in Cr/Sc multilayers

N. Ghafoor, F. Eriksson, P.O.Å. Persson, L. Hultman and J. Birch

Thin Film Physics Division, Department of Physics, Chemistry, and Biology (IFM) Linköping University, S-58183 Linköping, Sweden

Abstract

Nano-structural evolution of layer morphology and interfacial roughness in Cr/Sc metal multilayers grown with ion assistance during magnetron sputter deposition has been investigated by high resolution transmission electron microscopy and hard X-ray reflectivity. Calculations based on a binary collision model predict an ion-assisted growth window for optimized Cr/Sc multilayer interface sharpness, within the ion energy range of 21 eV to 37 eV and an ion flux of 10 ions per deposited atom. Multilayers with nominal modulation periods in the range of 1.6 nm to 10.2 nm, grown with these conditions, exhibit a well-defined layer structure with an improved flattening and abruptness of the interfaces. It is shown that multilayers with a modulation period smaller than 3.4 nm have clear benefit from the reduced intermixing obtained by utilizing a two-stage ion energy modulation for each individual layer. The amorphization of Sc and Cr layers, below certain thicknesses, is found to be independent of the low energy ion-assistance. It is also shown that the Cr/Sc multilayers, containing periods less than 2 nm are 'self healing' i.e. they re-gain abrupt interfaces and flat layers after morphological disturbances during ion assisted growth. In comparison, multilayers grown without ion-assistance exhibited severe roughness and layer distortions.

Keywords: Multilayers; X-ray mirrors; Ion assistance; Magnetron sputtering; Cr/Sc multilayers; Interface engineering; Optical coatings; Surface roughness

1. Introduction

Interface roughness evolution during growth of multilayers, one of the most important issues for X-ray optics and magnetic materials applications, has been addressed with both theoretical insight [1] and technological perspective [2]. However, state-of-the-art physical vapor deposition (PVD) technology of multilayers remains insufficient to achieve atomically abrupt and flat interfaces for nm to sub-nm thick layers in most material systems. The multilayer performance in almost all applications is limited by interface imperfections, collectively expressed as an interface width, σ. Providing a low intrinsic chemical reactivity and miscibility of the multilayer constituents, the interface structures and associated roughness primarily depends on the growth process. It has previously been realized that during PVD growth processes control of low-energy ions with appropriate mass and energy can modify the growth kinetics and yield films with low defect densities and smooth surfaces [3].

Brice et al. [4] studied ion-assisted growth of Ge, Si and C lattices by using an analytical model based on the binary collision approximation. They predicted an energy-window where momentum-energy transfer of ions causes only surface lattice displacements, to enhance the ad-atom surface mobility, while avoiding lattice displacements in the bulk. Nonetheless, for sub-nm sized multilayers, the surface displacements inevitably lead to a minimum of ± 1 monolayer intermixing at the boundaries of two materials. In practice, this small amount of intermixing can substantially affect the performance, for instance, reflectance of short period (Λ) soft X-ray multilayer mirrors. These effects were observed during growth of Cr/Sc and Ni/V multilayer mirrors intended for normal-incidence soft X-ray optics [5] and [6]. Recently, we introduced a technique using a modulated low-energy high flux ion assistance growth, where the ion energy is modulated within each individual layer during deposition [6]. The advantages of this method were seen in substantial enhancements of both soft and hard X-ray reflectivities (XRR) for short period, $\Lambda < 1.7$ nm, multilayers. Magnetron sputtering growth processes have thus been optimized both for layer thicknesses and corresponding ion energies for each part of the individual layers for different material systems. The highest near-normal incidence reflectivities of 20.7%, 2.7% and 2.1% were reported for the metal-layer systems Cr/Sc, Ni/V and Cr/Ti, at the Sc, V and Ti absorption edges, respectively [5-7]. In comparison, for instance, Cr/Sc multilayers grown with continuous low-energy high flux ion assistance showed a reflectivity of only 14.5% at the Sc absorption edge [8]. A theoretical verification of the concept of modulated ion assistance was independently presented by Zhou and Wadley [9]. They performed molecular dynamics simulations for a modulated low-energy ion assistance growth of metal Ni/Cu/Ni layers and obtained similar conditions for flat and chemically abrupt interfaces as in our studies.

While XRR, the most commonly used analysis technique for multilayers, is very effective in assessing the average structural nature of the multilayers, transmission electron microscopy (TEM) is one of a few direct probing techniques capable of structural investigations of individual layers. This technique has been used to reveal additional growth process induced effects on the structure of multilayers, such as columnar growth due to limited adatom mobility [10] and [11] and ion induced roughening/mixing [11] and [12]. For some metals in multilayers, such as e.g. Cr, Sc, Mo, Ni etc., an amorphous to crystalline transition has been observed by TEM for certain threshold bi-layer thicknesses [13] and [14]. The Cr/Sc multilayer system is considered very promising for near-normal incidence X-ray mirrors in the water window [15] and [16] and, therefore, was chosen for this study. For Cr/Sc multilayers, threshold thicknesses are found to be less than 1 nm for both materials [13] and [17]. Above the threshold thickness a polycrystalline growth of bcc-Cr and fcc-Sc grains with preferred orientation in the growth direction has also been reported [12]. Beyond these reports, however there is a limited knowledge of the dependence of nucleation, growth, microstructure, and interface structure for short period multilayers in particularly in conjunction with ion assisted growth.

In this work we apply TEM and XRR to address the above mentioned issues to: (i) clarify whether the amorphous growth is an effect of the layer thickness only or if the observed threshold thickness can be extended or suppressed using ion assistance of appropriate energy and flux, (ii) explore the evolving roughness in multilayers with thin and thick periods, (iii) investigate the structural dependence of multilayer period on the preceding roughness, and (iv) verify the structural growth model of the modulated growth mode, as predicted by theoretical simulations and suggested by XRR data [5], by comparing with lattice resolved electron microscopy images.

2. Theoretical considerations

For the ion-assisted growth of Cr/Sc multilayers, the impact of ion energy/momentum on the interfacial abruptness can be estimated in terms of lattice displacements caused by bombarding ions with a definite energy and flux. We made calculations based on a binary collision approximation in the ion-energy range 0 eV to 100 eV for both materials. A detailed description of the model can be found elsewhere [6]. For the calculations, the input parameters are; energy (E) and mass of the bombarding Ar ions, surface displacement energies ($E_d^{(s)}$), bulk displacement energies ($E_d^{(b)}$), and the masses of Cr and Sc atoms. In the calculations it is assumed that the bulk displacement energy is proportional to the cohesive energy of the elements and, owing to the lower coordination number of surface atoms, the surface displacement energies are assumed to be half of the bulk displacement energies, i.e. $E_d^{(s)} = 0.5\ E_d^{(b)}$.

The outcome of the calculations are shown in Fig. 1 where the energy deposited per Ar ion causing surface (upper curves) and bulk displacements (lower curves) of Cr (dashed curves) and Sc (solid curves) are plotted versus the ion kinetic energy. The surface displacement energies are indicated by horizontal dashed lines. Depending on the energy of the bombarding ion three different regions can be distinguished where there are: (I) no displacements, (II) primarily surface displacements, and (III) mixed surface and bulk displacements. In region (I) the ion energies are insufficient to cause any lattice displacements leading to a kinetically restricted arrangement of the arriving adatoms with an uneven or rough surface. Above the surface

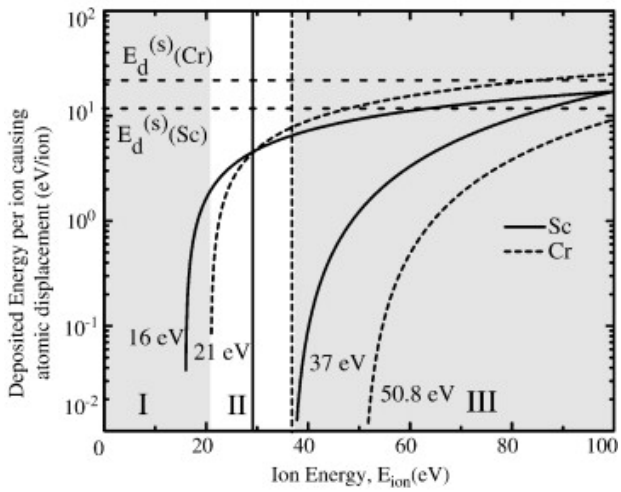

Fig. 1. Energy deposited per Ar ion causing atomic displacements in the surface (upper curve pair) and in the bulk (lower curve pair) for Cr (dashed line) and Sc (solid line). The surface displacement energies, $E_d^{(s)}(Sc)$ = 10.5 eV and $E_d^{(s)}(Cr)$ =11.1 eV, are shown as horizontal dashed lines. Different regions of ion energy transfer are indicated: (I) no displacement, $E_{ion} \leq$ 21 eV, (II) primarily surface displacement, E_{ion} = 21 eV to 37 eV, and (III) mixed surface and bulk displacement $\geq$ 37 eV. The optimized ion energies used during deposition of Cr/Sc multilayers are shown with vertical lines at $E_{ion}(Sc)$ = 29 eV and $E_{ion}(Cr)$ = 36 eV, respectively.

displacement threshold energies, region (II) and (III), adatoms may possess sufficient surface mobility to move on the surface and bond to high energy sites, like surface vacancies and steps, thus promoting a smoother surface. However, in order to preclude bulk damage it is imperative to stay below the bulk displacement threshold energies in region (III), which otherwise will cause intermixing of the interfaces. Thus, during ion-assisted deposition of Cr/Sc multilayers, smoother interfaces can be expected when Ar ion-energies higher than 16 and 21 eV, but lower than 37 and 51 eV are used for Sc and Cr, respectively. In other words, region (II) constitutes an ion-energy-window, from 21 eV to 37 eV, which is a good starting point for further optimization of deposition parameters for sharp and abrupt interfaces. The two vertical lines at 29 eV and 37 eV in Fig. 1 represent optimized ion energies for Cr and Sc, respectively, which were

experimentally used during Cr/Sc multilayer deposition. Due to the relatively low energy deposited per atom as surface displacement of the surface atoms, about 1/10th of the $E_d^{(s)}$, the calculations suggest that a high relative ion flux, about 10 times the flux of deposited metal atoms, is needed in order to displace each deposited atom at the surface before it is buried by other material. Hereafter, the relative ion flux parameter is described as an ion-to-metal flux ratio (Φ).

It is worth mentioning here that, although multilayer fabrication within the proper ion-energy window may generate abrupt interfaces, the probability of intermixing on an atomic scale at each interface cannot be neglected. This can only be avoided by minimizing the kinetic energy of the adatoms during formation of the interfaces, which is the fundamental idea of the modulated ion-assisted growth of each layer as described above.

3. Experimental details

Cr/Sc multilayers intended for interface investigation were deposited in a dual-cathode DC magnetron sputter deposition system. The 75 mm diameter magnetrons have opposite unbalanced type-II magnetic configurations. The essential attributes of the system are the independent control of ion energy and ion flux to the growing surface along with very fast acting shutters. A magnetic coupling of the outer poles of the magnetrons with each other and with a separate solenoid surrounding the substrate establishes magnetic field lines as guiding paths for secondary electrons from the cathodes to the substrate vicinity. The electrons increase ionization of the sputtering gas and therefore also Φ_{Cr} and Φ_{Sc}, at the growing film surface. The energies E_{ion}(Cr) and E_{ion}(Sc) of the impinging ions during growth of Cr and Sc, respectively, are controlled through an applied substrate bias potential in relation to the plasma. Both $\Phi_{Cr,Sc}$ and E_{ion}(Cr, Sc) were quantified from deposition rates and electrostatic probe measurements. The details of these measurements and analyses are described elsewhere [6]. All films were deposited at an ambient temperature on Si(100) substrates in an Ar atmosphere of 3 mTorr (0.4 Pa) with a background pressure of $2 \cdot 10^{-7}$ Torr ($2.66 \cdot 10^{-3}$ Pa).

For TEM imaging, cross-sectional specimens were prepared by conventional mechanical polishing followed by Ar ion etching at 5 keV. Finally, the specimens were subject to Ar ion etching at 2 keV to remove surface damage resulting from the previous step. The TEM investigations were performed using an FEI Tecnai G2 TF 20 UT field-emission TEM operated at 200 keV for a point resolution of 0.19 nm.

To facilitate the TEM investigation of the structural dependencies of multilayers with respect to the underlying roughness, a multilayer design was made in which seven multilayers (ML) of four different nominal periods, each with equal total thicknesses of 68 nm, were stacked on top of each other. Fig. 2 schematically illustrates the stacking order of ML's and in Table 1 the multilayer period (Λ) and the number of periods (N) for each stack are described. The choice of the initial multilayer period, Λ = 1.7 nm, matched the layer periodicity requirement for normal-incidence X-ray reflectivity at the Sc absorption edge. The consecutive periodicities were chosen to be 2, 4, and 6 times the period of the first multilayer (i.e., Λ = 3.4 nm, 6.8 nm, and 10.2 nm). The sequence was then mirrored and thus the initial period was deposited as the topmost multilayer. A Cr capping layer of 20 nm was also added on top of the stacked multilayer in order to avoid surface oxidation. A layer thickness ratio of Γ = 0.5 was chosen which yielded equally thick individual layers of Cr and Sc in all multilayers. Following this design, a series of three stacked multilayer samples A, B, and C were realized by using the deposition conditions according to:

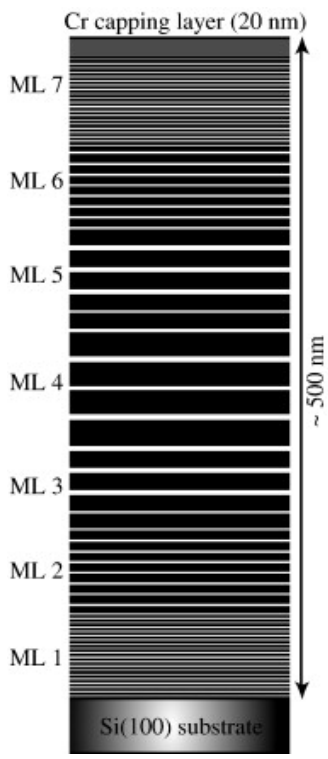

Fig. 2. Illustration of the Cr/Sc multilayer design the for TEM investigations. In a single sample seven periodic multilayers are stacked on top of each other with a layer thickness ratio of Γ = 0.5 and a total thickness of 68 nm. A Si(100) crystal was used as a substrate and a 20 nm thick Cr capping layer was grown on top. The multilayer period and the total number of bilayers in each individual multilayer are given in Table 1.

Table 1: Multilayer period, Λ, and number of periods, N, used for different stacks (ML) in the multilayer design

Multilayer (ML)	Multilayer period Λ (nm)	Number of periods N
1 and 7	1.7	40
2 and 6	3.4	20
3 and 5	6.8	10
4	10.2	5 or 6

3.1. Low flux, low energy ion assistance

The first stacked multilayer structure "sample A" in this sample series was deposited without any intended ion assistance. Technically, the substrate was kept at a floating potential and no magnetic coupling was used between the magnetrons and the substrate solenoid. As expected, relatively low ion-to-metal flux ratios of Φ_{Cr} = 0.5 and Φ_{Sc} = 0.8 were found for Cr and Sc, respectively. The ion energies were calculated [6] by measuring the substrate floating potential, V_f, and the plasma potential, V_p, and were found to be E_{ion}(Cr) = 5.5 eV and E_{ion}(Sc) = 3.5 eV, respectively.

3.2. High flux, continuous energy ion assistance

The second stacked sample "sample B" was deposited with a low-energy, high-flux ion-assistance. A comparatively high ion flux of the sputtering gas was achieved at the growing film by coupling the magnetic field of the magnetrons with the in-situ solenoid surrounding the substrate. The ion-to-metal flux ratios were measured to Φ_{Cr} = 4 and Φ_{Sc} = 8 for Cr and Sc, respectively, i.e. about 10 times higher than without the solenoid. Moreover, the kinetic energies of the impinging ions were raised to E_{ion}(Cr) = 36 eV and E_{ion}(Sc) = 29 eV, respectively, by applying a − 30 V bias to the substrate. The choice of these ion energies was based on previous optimization studies for Cr/Sc multilayers mirrors [5].

3.3. High flux modulated energy ion assistance

For the third stacked sample "sample C", the modulated ion-assisted growth was applied for each individual layer of Sc and Cr, keeping the magnetron solenoid coupling the same as for the continuous ion assistance. Here the first 0.3 nm of each individual layer was deposited with grounded substrate (giving an ion energy of E_{ion}(Cr) = 4 eV during Cr layer deposition and electron irradiation of E_e(Sc) = 1.5 eV during Sc layer deposition) and the remainder of each layer was then deposited with energetic ions of E_{ion}(Cr) = 36 eV and E_{ion}(Sc) = 29 eV,

respectively. The values of initial thickness and ion energies were obtained from previous process optimizations [5].

In addition to the stacked multilayer series for TEM analysis, nine single multilayers of bilayer periods of 1.6 nm, 3.2 nm and 6.4 nm were also grown with the above mentioned schemes. Hard X-ray (Cu-K_α) reflectivity was performed on these single multilayers and complementary information to electron microscopy in terms of layer definition and/or interfacial roughness variations was obtained.

X-ray reflectivity (XRR) and X-ray diffraction were performed using a Philips MRD diffractometer in a parallel beam configuration with a line-focused copper anode source (Cu-Kα, E = 8046 eV), operating at 0.8 kW. A Ni β-filter and a fixed divergence slit of 1/32° was used to condition the primary beam and in the secondary beam path the central channel of a 0.3° parallel plate collimator was used together with a flat graphite crystal monochromator. A proportional detector was used for the data acquisition.

4. Results and discussion

In Fig. 3 peak intensities of multilayer reflections determined from XRR scans of single multilayers are plotted versus the scattering angle, 2θ. The comparison is made for the three different ion assistance schemes, and Fig. 3(a)–(c) shows the result for multilayers with different modulation periods; (a) Λ = 1.6 nm, N = 100 (b) Λ = 3.2 nm, N = 50, and (c) Λ = 6.4 nm, N = 25. From the thinnest multilayer period of 1.6 nm (Fig. 3(a)), reflections up to the third order were recorded for the multilayers deposited with modulated and continuous ion assistance, while only the first reflection, with very low peak intensity, was measured for the multilayer grown with no ion assistance. A poor layer structure due to limited adatom mobility in the absence of ion assistance is the probable explanation for this single low intensity reflection. It is also clear that for very thin layers of Cr and Sc, here ~0.8 nm, modulated ion assistance is advantageous over continuous ion assistance as all three measured peaks show significantly higher intensities. Also, the difference in peak intensities for all reflection orders for thicker layers (Λ = 3.2 nm and Λ = 6.4 nm) depicts a positive influence of ion energy modulation (Fig. 3(b) and (c)). Multilayers with thicker periods generally exhibited lower intensities and fewer orders of reflections when grown without ion assistance. These qualitative observations are in accordance with the expected effects of the three investigated ion assistance schemes and indicate a flattening, thanks to ion assistance, and a reduced mixing of the interfaces when the ion assistance is switched off at the onset of each deposited layer for all investigated Λ. Thus,

modulated ion assistance provides for an abrupt compositional modulation with an increased intensity of the X-ray reflections as a consequence.

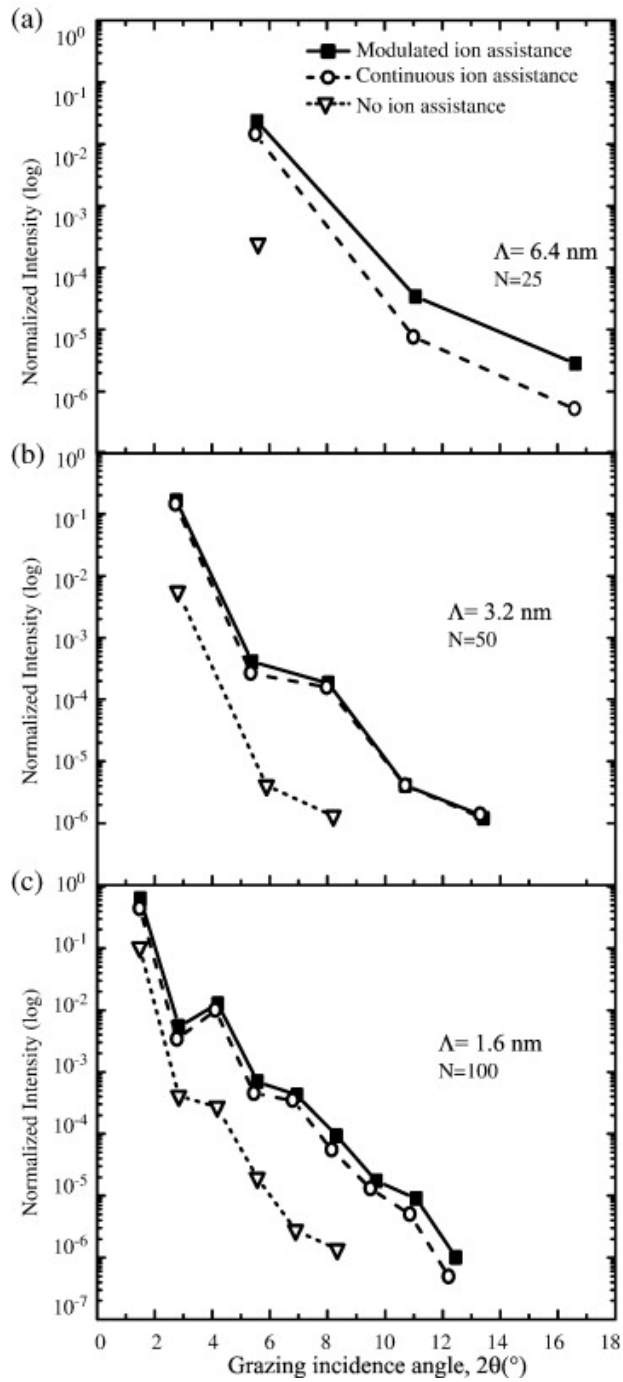

Fig. 3. Plots of measured X-ray reflectivity (Cu-K_α) peak intensities of multilayers reflections (Bragg order) for 9 single multilayers grown with varying ion assistances. Plots are separated for multilayers deposited with different layer periodicities as, (a) Λ = 1.6 nm, (b) Λ = 3.2 nm and (c) Λ = 6.4 nm.

Fig. 4 shows cross sectional overview TEM images from the three stacked multilayers grown with the different ion assistance schemes. Sample A, grown without any ion-assistance, i.e. with limited growth kinetics, is shown in Fig. 4(a) and exhibits a columnar and rough layered structure. There are also inter-columnar voids due to the presence of self-organized growth mounds, separated by deep surface trenches, in combination with atomic shadowing [18] and [19]. This surface roughness exhibits strong vertical correlation once it has been established and evolves into columns extending to the top of the Cr capping layer. It can be seen in Fig. 4(a) that the roughness evolution increases with increasing Λ and, interestingly, for the top multilayers deposited with a decreasing Λ the roughness evolution is retarded effectively giving rise to a smoothening effect. It is also important to note that the individual bilayers are visible even in the top-most multilayer of the stack with the thinnest Λ = 1.7 nm. This shows that the local abruptness of the interfaces is not significantly deteriorated by the roughening of the surfaces. Hence, we conclude that the major concern with this material system as X-ray mirrors is the roughness evolution rather than intermixing or interdiffusion when grown at ambient substrate temperatures. A polycrystalline nature of the layers with Λ ≥ 3.4 nm is evident from the appearance of dark diffraction contrast, revealed primarily in the Cr-layers which is in agreement with the previous observations [13].

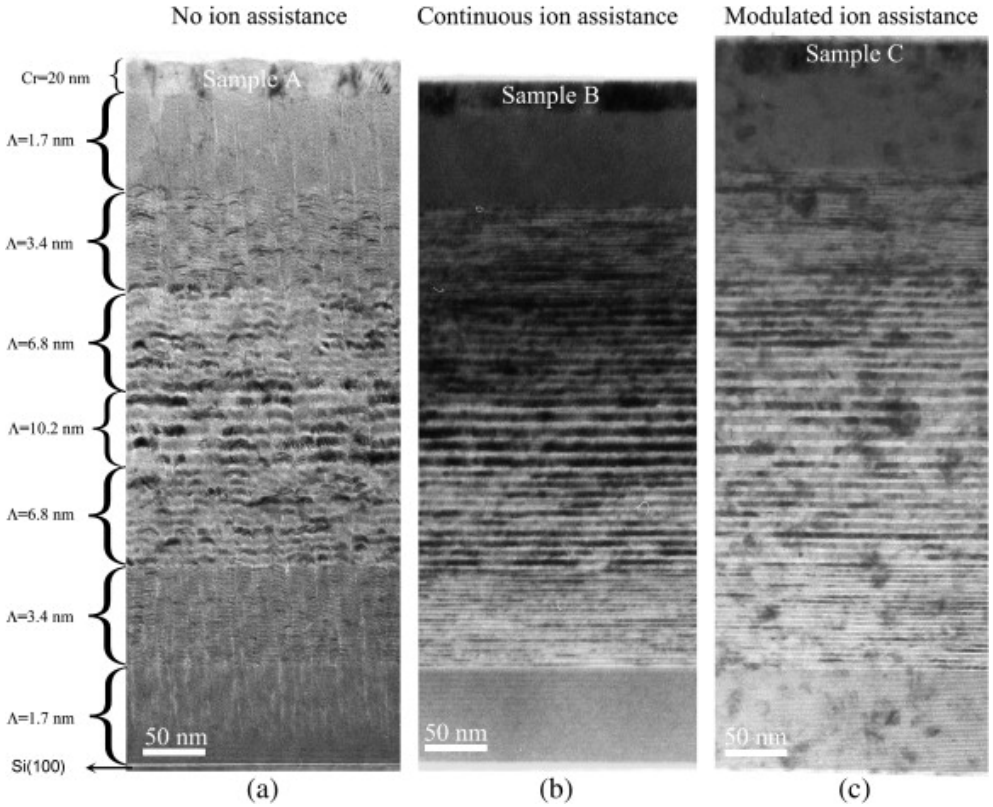

Fig. 4. Cross-sectional TEM overview micrographs for Cr/Sc multilayers samples A, B and C consisting of multilayers with bilayer periods (1.7 nm; 3.4 nm; 6.8 nm; 10.2 nm) deposited in increasing and decreasing order (ML 1 through ML 7, respectively) under three different deposition conditions: (a) no ion assistance, (b) continuous ion assistance, and (c) modulated ion assistance. In all images the Cr layers exhibit dark contrast.

A dramatic improvement with respect to roughness evolution of the multilayers is evident from the overview TEM image of sample B in Fig. 4(b). This multilayer, which was grown with enhanced ion flux and with continuous ion energy shows flat and distinct layers throughout the film without the columnar growth. A homogeneous contrast is observed in the layers with $\Lambda \geq 3.4$ nm, which suggests a more homogeneous arrangement of the atoms within each layer than when no ion assistance was used. The grains can more clearly be seen in Cr layers (dark contrast).

The micrograph in Fig. 4(c) shows an overview cross-section of sample C where the stacked multilayer was grown with modulated energy ion assistance. The major attributes that can be seen at this relatively low magnification, are the smooth and abrupt interfaces of at least the same quality as for the sample B grown with continuous energy ion assistance. Moreover, for $\Lambda \geq 3.4$ nm, grains are better defined and the average lateral grains size, mainly in the Cr layers, is somewhat reduced.

To reveal differences in atomic layer arrangements at the interfaces high resolution TEM (HRTEM) was performed at identical focus conditions (Scherzer defocus $\Delta f = -42$ nm as measured from the Fourier transform and at $\Delta f = -100$ nm for the thinnest layers in order to promote image contrast in these layers). Fig. 5 shows lattice resolved HRTEM images from the individual multilayers with the thinnest bilayer periods of 1.7 and 3.4 nm, both from the bottom (ML 1 and ML 2) and when repeated at the top of the films (ML 7 and ML 6), for the different samples. The Sc and Cr layers can be distinguished (bright and dark, respectively) in all three samples. In sample A, a distorted layer structure is seen in all four stacks. In samples B and C, deposited with a high-flux of low-energy ions, independent of energy modulation, an abrupt difference in mass contrast is seen which shows a positive influence of ion assistance for producing distinct interfaces and smooth layers.

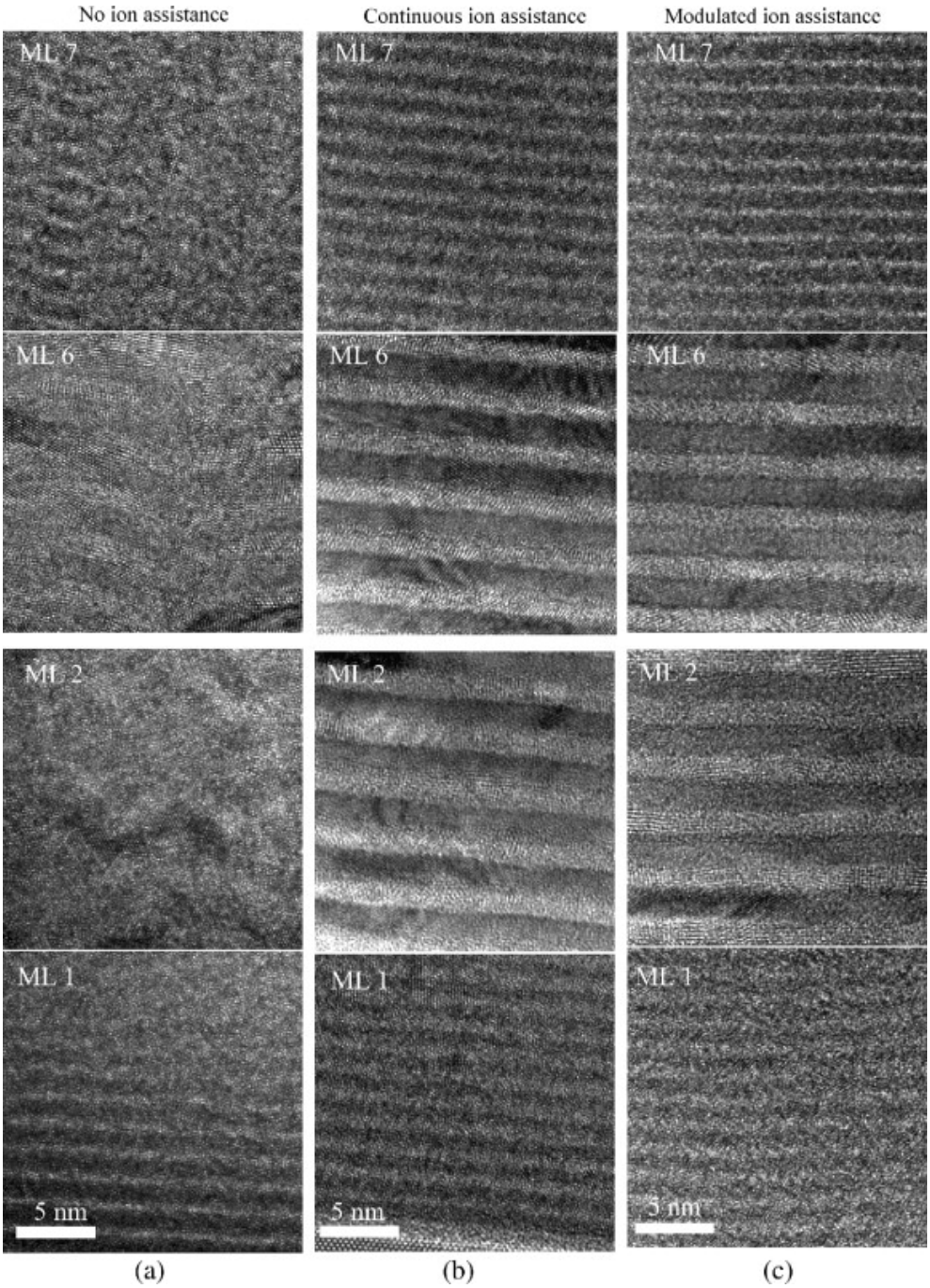

Fig. 5. HRTEM images of the bilayer periods, Λ = 1.7 nm (ML 1 and ML 7) and Λ = 3.4 nm (ML 2 and ML 6), for the three different growth conditions.

As judged from the images in Fig. 5, both Sc and Cr layers in the Λ = 1.7 nm ML's are amorphous, independent of the growth order, i.e., whether they were grown on the native oxide of the Si substrates or on the top of the polycrystalline second last multilayer (ML 6). The two

metals are in an amorphous state in both ML 1 and ML 7 in all three samples, i.e., independent of ion-assistance scheme as well as position in the stack. We thus infer that the amorphization is not primarily an ion-surface interaction effect. Amorphization of pure metals is a rare phenomenon and would require quenching rates far in excess of what the present vapor phase deposition process is providing at ambient temperature. The explanation should rather be sought in a lowering of the total free energy by elimination of high energy non-coherent crystalline interfaces between the bcc-Cr and hcp or fcc [12] -Sc through the amorphization process. Another possibility could be an interaction of residual gas under the present high-vacuum conditions with the condensating sub-nm Cr and Sc layers. Initial composition analysis by elastic recoil detection analysis showed the presence of up to 4.7 at.% of O, 0.8 at.% N and 0.7 at.% of C impurities in these samples. These elements may interact strongly with refractory metals, forming molecular non-metallic species with low adatom mobility and directional bonds, effective to promote renucleation and thus yield the apparent amorphization of the initial atomic layers.

When continuous ion assistance is employed, due to ion induced atomic surface displacements, by low energy ion bombardment, on a completed layer when the growth of the next layer is commenced, an intermixed interface will inevitably be formed. For amorphous layers with $\Lambda <$ 3.2 nm where no crystallite facets (giving rise to roughness) are anticipated at the interface, this intermixing leads to an interface width of at least two atomic diameters, 0.3 nm, which is in good agreement with X-ray reflectivity simulations [8]. In the case of modulated ion assistance, no ion energy is set for the first 0.3 nm of growth of each layer, which, according to our calculations in Fig. 1 and plasma probe measurements, does not provide ions with high enough energy to induce surface displacements and therefore minimizes the adatom mobility. This allows for abrupt interface formation during the initial growth while the ion energies during the subsequent deposition of the remaining part of each layer are not high enough to cause any interface mixing by bulk displacements, but will enhance the surface mobility and increase the surface smoothening.

Another very interesting effect that can be observed in the stacks grown with high flux and low energy ion assistance is the good layer definition with flat layers and abrupt interfaces in ML 7 with $\Lambda = 1.6$ nm (Fig. 4(b) and (c)) even though they were grown on top of 6 other multilayers with thicker bilayer periods, some of them being far from perfect with pronounced roughness. This shows that Cr/Sc multilayers with ultra-short periods are 'self healing' with respect to morphological disturbances during the film growth. This is a combined effect of the amorphous microstructure, which does not inherit crystalline features from one layer to the next, and the stimulated adatom mobility during ion assisted growth resulting in smoother surfaces due to less

atomic shadowing. This behavior may be one strongly contributing reason to the successful application of this material system as soft X-ray mirrors.

Multilayers grown with ion assistance with Λ = 3.4 nm (ML 2 and ML 6), are polycrystalline with crystallite sizes limited to the layer thickness of Sc and Cr in the vertical direction, as seen in Fig. 5. Laterally, the crystallites may extend up to 100 nm as was estimated from the TEM lattice resolved images. There is also a difference in the interface abruptness between the two ion-assisted growth processes. This can be seen by the appearance of Fresnel fringes (dark/bright lines) along the interfaces. More abrupt interfaces result in fringes of strong contrast. The continuous ion assistance produced diffuse interfaces between the layers while the modulated ion-assistance gave sharper interfaces. The diffuse interfaces obtained with continuous ion bombardment can be explained by surface displacement events lead to intermixing, in accordance with the ion-energy calculations. In comparison, Λ = 3.4 nm multilayers grown without ion-assistance exhibited much smaller lateral crystallite sizes due to the limited adatom mobility during growth of those multilayers, which also is the cause of the observed severe roughness and layer distortions. However, the contrast visible in these layers in the low magnification image in Fig. 4(a) is indicative of diffraction effects and hence implies crystalline components also when no ion-assistance was used, showing that crystallization is not primarily ion-induced bur rather an effect of the layer thicknesses.

The multilayers with the large modulation periods of Λ = 6.8 nm (ML 3 and ML 5) and Λ = 10.2 nm (ML 4) are shown side by side in Fig. 6 for samples B and C, grown with ion assistance. Both the Sc and Cr layers are clearly polycrystalline, but a higher structural order can be seen in the crystallites of the multilayers grown with modulated ion assistance. Lattice fringes can be observed locally to extend over the thickness of individual Sc and Cr layers. Fast Fourier transform analyses of the lattice resolved images indicated that the Sc crystallized in a cubic structure which is in agreement with the previous observations of Gorelik et al. [12]. However, we could not identify any epitaxial relationships between the Cr and Sc layers, as they did. This difference can be due to the differences in ion-assistance schemes, ion energies, as well as ion fluxes. An absence of epitaxial growth may be expected when the adatom mobility is very low which limits the possibility for the nuclei to re-arrange to fit any template structure. This is the situation to be expected in our films grown without ion assistance and, as seen in Fig. 4(a), such conditions also results in very distorted crystalline lattices. In the films grown with modulated ion-assistance, the initial 0.3 nm of each layer were deposited without ion-assistance to form as abrupt interfaces as possible. Thus, we can expect the same inability of the nuclei to re-arrange as in the case of no ion assistance and the 0.3 nm thick, highly disordered, initial layer can be expected to hinder epitaxy. The multilayers investigated in Ref. [12] were grown with continuous relatively high energy (about 100 eV), Ar-ion assistance with a low ion-to-neutral

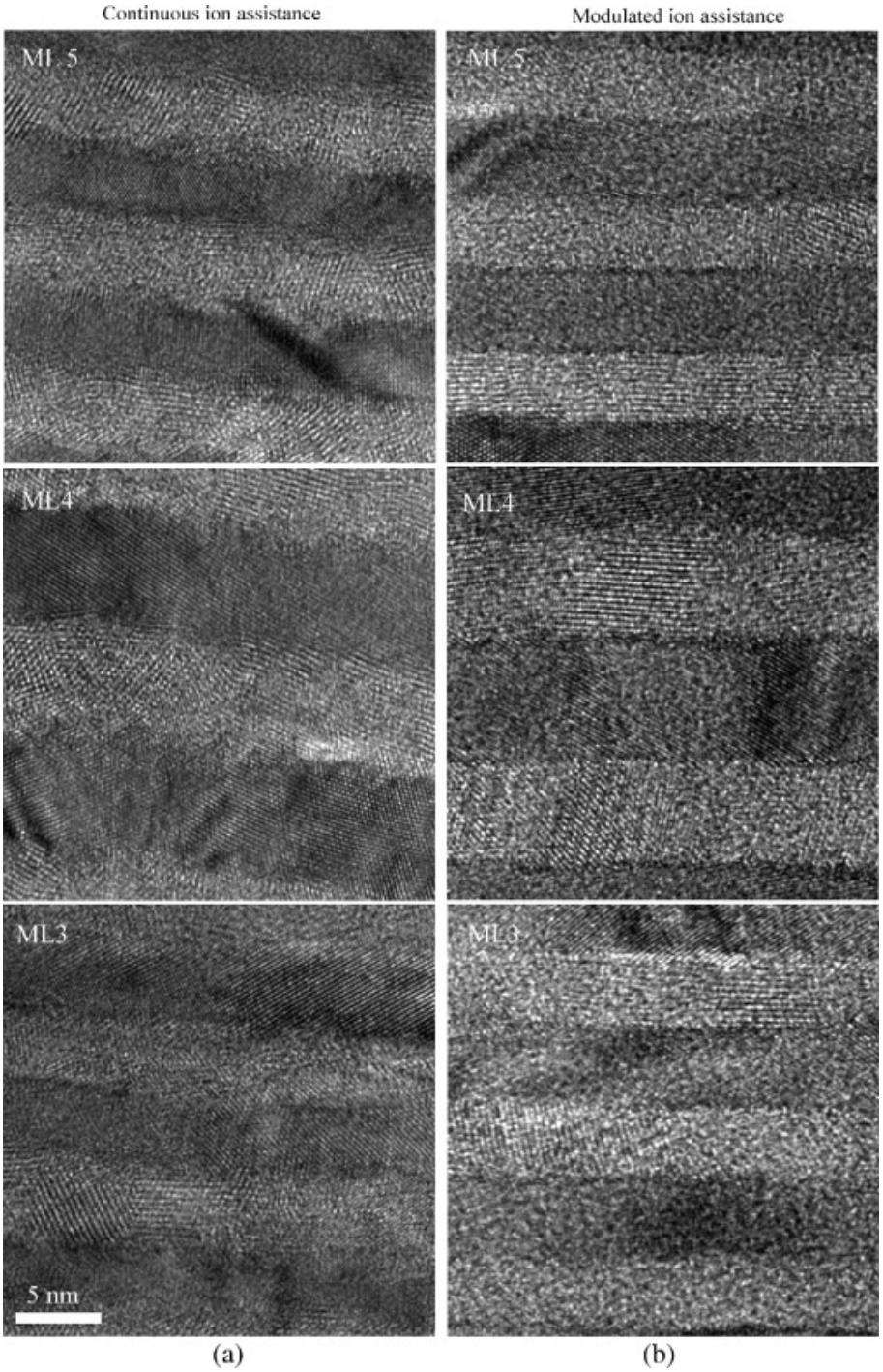

Fig. 6. HRTEM images from the bilayer periods Λ = 6.8 nm (ML 3 and ML 5) and Λ = 10.2 nm (ML 4), for the sample B grown with a continuous (a) and for sample C grown with a two-stage modulated ion-assistance (b).

flux ratio (balanced magnetrons). Therefore, the film nucleation and the establishment of epitaxy in their case are different from our growth situation even when continuous ion-assistance was used. However, by comparing the TEM images in Ref. [12] to those shown in Fig. 5, we can note that our samples grown with continuous ion assistance exhibit more diffuse interfaces, more distorted crystal lattices, as well as frequent moiré fringes in the darker Cr-layers which indicate a presence of overlapping of misoriented crystallites.

A general observation from the TEM image analysis of all Λ is that an improved interface definition is achieved by implementing modulated ion assistance which is in qualitative agreement with the X-ray reflectivity shown in Fig. 3.

5. Conclusion

It is shown that a significant improvement in interface abruptness and flatness can be achieved in Cr/Sc multilayer thin films by independent variation of ion energy and ion-to-metal flux ratio during magnetron sputter deposition. Specifically, the concurrent bombardment of high-flux of low-energy ions, predicted by theoretical modeling, during growth can be employed to overcome columnar and rough layer growth in the multilayer system. A significant flattening with distinct interfaces for a range of bilayer periods (Λ = 1.6 nm–10.2 nm) was obtained by implementing a flux $\Phi_{Cr} = 4$ and $\Phi_{Sc} = 8$ with energy of 21 eV < E_{ion} < 37 eV. Moreover, it is shown both by XRR and TEM analyses that newly implemented modulated ion assistance during growth of each individual layer of Sc and Cr has a pronounced positive effect on the interface quality in terms of reduced intermixing for Λ = 1.6 nm–10.2 nm. This processing was realized by using a $E_{ion}(Cr) = 4$ eV and $E_{ele}(Sc) = 1.5$ eV during deposition of the first 0.3 nm of each individual layer and then applying $E_{ion}(Cr) = 36$ eV and $E_{ion}(Sc) = 29$ eV, respectively, for the remaining layer. A scheme is thus presented for the selection of initial layer ion energies. However, the optimization of initial and final ion-energies and thicknesses must be done for each specific layer material and thickness.

It is further demonstrated that independent of ion assistance scheme, amorphous layers of the two materials form for bilayer periods below 3.4 nm. It is inferred that the amorphization for these layers is an interface effect due to a higher free energy associated with crystallized interfaces and/or interaction with a residual gas in the vacuum system. The results have impact for implementing modulated two-stage ion assistance multilayer deposition of general materials systems.

References

[1] S.K. Sinha, E.B. Sirota and S. Garoff, Phy. Rev., B 38 (1998), p. 2297.

[2] T. Kingetsu and M. Yamamoto, Surf. Sci. Rep. 45 (2002), p. 79.

[3] I. Petrov, P. Barna, L. Hultman and J.E. Greene, J. Vac. Sci. Technol., A, Vac. Surf. Films 21 (2003), p. 117.

[4] D.K. Brice, J.Y. Tsao and S.T. Picraux, Nucl. Instrum. Methods Phys. Res., Sect. B 44 (1989), p. 68.

[5] F. Eriksson, PhD Thesis, Linköping Studies in Science and Technology, No. 875, ISBN: 91-7373-950-2, ISSN: 0345-7524, Sweden 2004.

[6] F. Eriksson, N. Ghafoor, F. Schäfers, E.M. Gullikson and J. Birch, Thin Solid Films 500 (2006), p. 84.

[7] N. Ghafoor, F. Eriksson, P.O.Å. Persson, F. Schäfers and J. Birch, Appl. Opt. 45 (2006), p. 137.

[8] F. Eriksson, E.M. Gullikson, G.A. Johansson, J. Birch and H.M. Hertz, Opt. Lett. 28 (2003), p. 2494.

[9] X.W. Zhou and H.N.G. Wadley, J. Appl. Phys. 87 (2000), p. 2273.

[10] E.E. Fullerton, I.K. Schuller and Y. Bruynseraede, Mater. Res. Bull. XVII (12) (1992), p. 33.

[11] K. Järrendahl, I. Ivanov and J.-E. Sundgren, J. Mater. Res. 12 (1997), p. 1806.

[12] T. Gorelik, U. Kaiser, T. Kuhlmann, S. Yulin and W. Richter, Appl. Surf. Sci. 230 (2004), p. 1.

[13] T. Kuhlmann, S. Yulin, T. Feigl, N. Kaiser, T. Gorelik, U. Kaiser and W. Richter, Appl. Opt. 41 (2002), p. 2048.

[14] S. Bajt, D.G. Stearns and P.A. Kearney, J. Appl. Opt. 90 (2001), p. 1017.

[15] N.N. Salashchenko and E.A. Shamov, Opt. Commun. 134 (1997), p. 7.

[16] F. Schäfers, H.-C. Mertins, F. Schmolla, I. Packe, N.N. Salashchenko and E.A. Shamov, Appl. Opt. 37 (1998), p. 719.

[17] E. Majkova, Y. Chushkin, M. Jergel, S. Luby, V. Holy, I. Matko and B. Chenevier, Thin Solid Films 497 (2006), p. 115.

[18] L. Hultman, L.R. Wallenberg, M. Shinn and S.A. Barnett, J. Vac. Sci. Technol., A, Vac. Surf. Films 10 (1992), p. 1618.

[19] J.-S. Chun, I. Petrov and J.E. Greene, J. Appl. Phys. 86 (1999), p. 3633.